




Carrier recombination dynamics in green InGaN-LEDs with quantum-dot-like structures

Ming Tian^{1,2}, Cangmin Ma¹, Tao Lin^{1,*}, Jianping Liu³, Devki N. Talwar⁴, Hui Yang³, Jiehua Cao¹, Xinying Huang¹, Wenlong Niu¹, Ian T. Ferguson⁵, Lingyu Wan^{1,2}, and Zhe Chuan Feng^{1,2,*} 

¹Laboratory of Optoelectronic Materials and Detection Technology, Center on Nanoenergy Research, Guangxi Key Laboratory for the Relativistic Astrophysics, School of Physics Science and Technology, Guangxi University, Nanning 530004, China

²State Key Laboratory of Luminescence and Applications, Changchun Institute of Optics, Fine Mechanics and Physics, Chinese Academy of Sciences, Changchun 130033, China

³Suzhou Institute of Nano-Tech and Nano-Bionics, Chinese Academy of Sciences, Suzhou 215123, China

⁴Department of Physics, University of North Florida, Jacksonville, FL 32224, USA

⁵Southern Polytechnic College of Engineering and Engineering Technology, Kennesaw University, Kennesaw, GA 30144, USA

Received: 5 July 2020

Accepted: 15 September 2020

Published online:

29 September 2020

© Springer Science+Business Media, LLC, part of Springer Nature 2020

ABSTRACT

Exciton localization phenomena are considered here to comprehend the high internal quantum efficiency in InGaN/GaN multiple-quantum-well structures having discrete quantum dots (QDs) prepared by metal–organic-chemical-vapor deposition method on *c*-sapphire substrates. Spectroscopic results from the variable-temperature steady-state-photoluminescence and time-resolved photoluminescence (TRPL) are investigated. While the exciton localization is enhanced by strong localized states within the InGaN/GaN QDs—the impact of free carrier recombination cannot be ignored. The observed non-exponential decay in TRPL measurements is explained using a model by meticulously including localized exciton, non-radiative and free carrier recombination rates. A new method is proposed to calculate the internal quantum efficiency, which is supplementary to the traditional approach based on temperature-dependent photoluminescence measurement.

Introduction

III-Nitride-based light-emitting diodes (LEDs) have attracted much attention in recent years due to their potential use in solid-state lighting, sensors, low

threshold lasers, etc. [1, 2]. Energy band gap tunability of InGaN with its prospective use as an active layer in LEDs has instigated both scientific and engineering interests for realizing full-color displays in the visible range. Based on these remarkable achievements, the 2014 Nobel Prize in physics was

Handling Editor: Kevin Jones.

Address correspondence to E-mail: taolin@gxu.edu.cn; fengzc@gxu.edu.cn

<https://doi.org/10.1007/s10853-020-05343-6>

awarded for GaN-related high efficient blue light-emitting diodes [3–5]. Consequently, the optoelectronic industry around the world is rapidly expanding where the III-N based quantum dots (QDs) [6], multi-quantum wells (MQWs) and/or superlattices (SLs) are being employed in LEDs, lasers, solar cells and medical imaging devices [7]. One must note that $\text{In}_x\text{Ga}_{1-x}\text{N}$ -based quantum wells (QWs) grown on c-sapphire with low In-contents ($x < 0.2$) exhibit high internal quantum efficiency (IQE) although GaN has excessive ($\sim 10^9 \text{ cm}^{-2}$) dislocation density—caused by lattice mismatch ($\sim 16\%$) between GaN and sapphire. The higher IQE is attributed to carrier localization phenomena occurring in the QD-like In-rich InGaN formed in the InGaN layer—the carrier localization reduces the effect of non-radiative recombination at the dislocations [8].

While the IQE in InGaN-based MQWs has a spectral range extending from blue to green wavelengths, it drops significantly for high In-contents due to the issues related to crystalline quality commonly known as a “green gap.” The green-gap effect is believed to be instigated by high dislocation density—resulting from the large lattice mismatch between InGaN and GaN. The dislocations lead to the increased nonradiative recombination rate and charge separation that arises from the enhanced piezoelectric polarization in the QW, preceding to the reduction in electron–hole wave function overlap [9–13]. To circumvent this problem inherent to InGaN MQWs—an alternative technique of fabricating nano-sized In-rich clusters in GaN layers (to act as light-emitter) has been suggested in the green and/or even longer spectral range.

These attempts of assimilating quasi-QDs in In-rich regions of InGaN active layers have significantly improved the low quantum efficiency. The possible reasons for the increase in IQE are: (1) the localized excitons that improve local crystalline quality [14, 15], (2) reduction in the built-in piezoelectric polarization field to steer the alleviation of quantum confinement stark effect (QCSE) [16–19], (3) decrease of non-radiative recombination rate of carriers caused by dislocations and related defects, and (4) shorter carrier lifetime and weaker Auger recombination. All these benefits have led to the great prospects of InGaN QDs for green and longer wavelength light-emitting devices [20, 21].

While the growth of InGaN QDs has been successfully achieved by metal–organic chemical vapor

deposition (MOCVD) or molecular beam epitaxy (MBE)—limited optical spectroscopy studies are available, however, to comprehend the microstructural and carrier transport properties. One of the most promising methods to study IQE is the time-resolved photoluminescence (TRPL). This method reveals the decay of PL emission leading to a deep understanding of the recombination process of carriers. An earlier study [22] on InGaN/GaN structures suggested the TRPL decay curves to be exponential due to exciton recombination. On the contrary, several recent studies [23, 24] in III-N MQWs have revealed non-exponential TRPL curves both at low- and higher temperatures. Morel et al. [23] offered a possible explanation that the non-exponential decay is due to a “pseudo-DAP” recombination. There are some reports attributing the non-exponential TRPL curves to fast and slow decays [24]. To the best of our knowledge, the exact mechanisms of emission and carrier transport in green QDs like structures are still controversial. Moreover, the free carrier recombination from InGaN/GaN QD-like structure has not been considered in the literature.

In this work, we report a comprehensive experimental and theoretical investigation on the carrier transport and luminescence mechanisms in MOCVD-grown InGaN/GaN MQWs containing discrete QD-like In-rich clusters, by using variable-temperature steady-state photoluminescence and TRPL methods. A novel theoretical methodology is established to simulate and analyze the IQE for realizing the non-exponential decay curves observed in TRPL measurements on InGaN/GaN QD structures without any extra prerequisite. Our study has strongly suggested that the free carrier recombination in MOCVD grown InGaN/GaN MQWs with discrete QDs plays an important role in the luminescent process.

Experimental

Sample growth

In Fig. 1a, a schematic diagram is shown for the epitaxially grown InGaN/GaN MQW structure by using the MOCVD technique. Trimethylgallium (TMGa) and Triethylgallium (TEGa) were used as precursor for Ga sources for growing GaN and InGaN layers, respectively. With H_2 or N_2 as a carrier gas, trimethylindium (TMIn) and ammonia (NH_3)

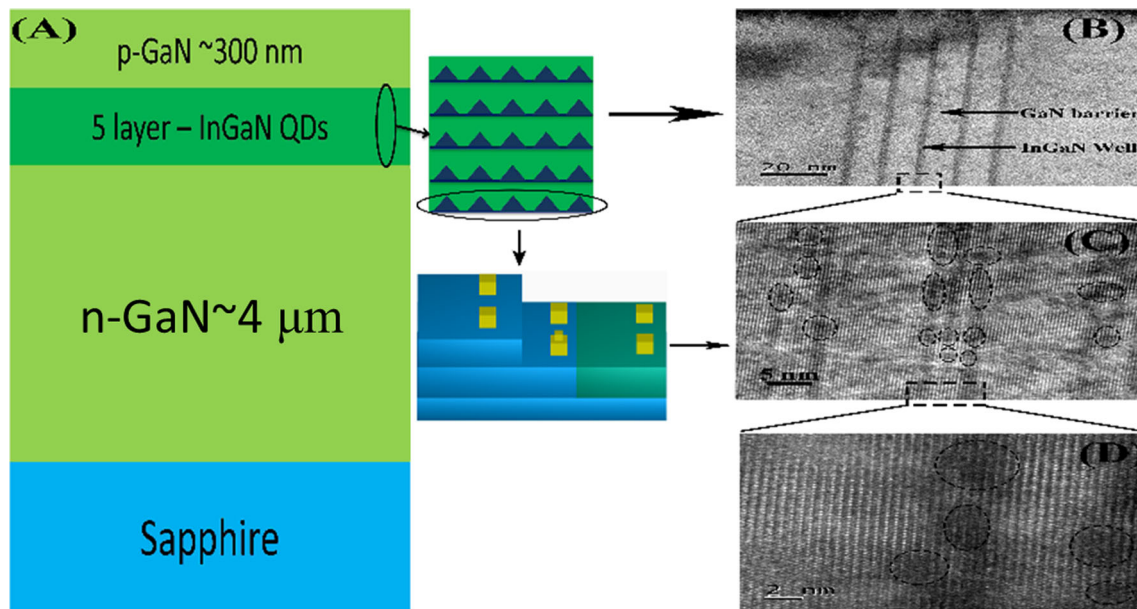


Figure 1 **a** Schematic illustration of the QDs sample on sapphire. **b** High resolution transmission electron microscopy image for InGaN/GaN QDs used in this work. **c** a magnification of the circled InGaN QD picture B. **d** a magnification of the circled InGaN well picture C.

were used as the precursors for In and N, respectively. The structure consists of a 4-μm-thick n-GaN buffer layer grown first on the c-plane sapphire substrate at about 670 °C, followed by five QW layers containing discrete InGaN QDs and a 300 nm-thick GaN capping layer. InGaN QDs were deposited at 670 °C with a molar TMI_n/(TMI_n + TEGa) gas phase ratio of about 1:2. The V/III ratio was set to 1.35×10^4 [25].

Our high-resolution transmission electron microscopy (TEM) images of InGaN QD sample were taken by FEI Tecnai G2 F20 TEM at an accelerating voltage of 200 kV and with an instrumental error of ± 0.24 nm. Figure 1b–d revealed an average width of the QDs and QWs as 2.4 nm and 4.5 nm, respectively.

Time-resolved photoluminescence measurements

The TRPL measurements were performed on MOCVD grown sample by varying temperature from 14 to 300 K. A pico-second laser diode (PDL 800-D) of wavelength 376 nm is used as the excitation source with 44 ps pulse-width and about 21.0 pJ laser pulse energy. The laser beam was focused on sample of about 100 μm. The PL spectral signals were detected by a photomultiplier tube connected to a 0.75 m spectrometer (Omini-λ750i, Zolix, China). The PL

decay spectra were collected by a time-correlated single-photon counting (TCSPC) system.

Results and discussion

Theoretical model

In the model established earlier [22], the exciton recombination in InGaN/GaN MQWs can be expressed as:

$$-\frac{\partial n}{\partial t} = An + A'n = \frac{n}{\tau} \quad (1)$$

where n represents the exciton density; $\tau = [1/(A + A')]$ is the carrier lifetime and the terms A , A' are, respectively the radiative and non-radiative recombination rates. So, An and $A'n$ are the radiative and non-radiative recombination exciton density, respectively. At a given temperature, if the density of localized exciton (n_{loc}) is proportional to the density of injected carriers ($n_{injected}$), i.e., $n_{loc} \propto n_{injected}/N_{loc}$ where N_{loc} represents the density of localized states. In this situation, n can be considered as the density of injected carriers—with the scale coefficient included in A .

In this model, it is implied that the localized exciton recombination dominates the whole radiative recombination process. Note that the “localized

excitons" represent the excitons that are localized on certain local potential minima induced by In-composition fluctuations or well thickness fluctuations. Specifically, one "localized exciton" may be a trapped electron and a coulombically bound hole, or a trapped hole and a coulombically bound electron. However, it is also known that the strong intrinsic electric fields in polar InGaN/GaN MQWs can cause the separation of the above coulombically bound electron and hole in the direction perpendicular to the plane of QWs. This suppresses the formation of exciton between electrons and holes [26], resulting in a deviation from the exciton recombination model described in Ref.[22].

In other studies, especially on electroluminescence (EL) properties of GaN LEDs, many researchers believed that there are three carrier recombination mechanisms in InGaN/GaN MQWs: (1) the Shockley–Read–Hall (SRH) non-radiative recombination, (2) the bimolecular radiative recombination, and (3) the Auger non-radiative recombination [27]. The processes are frequently characterized by carrier rate equation using $A'n$, Bn^2 and Cn^3 , respectively where A' , B , and C are the SRH, radiative, and Auger coefficients and n represents the carrier concentration [28, 29]. However, it has to be on the high injection condition (i.e., $n \geq 10^{18} \text{ cm}^{-3}$) that the intraband Auger recombination become considerable. Therefore, it is reasonable in our work to neglect the influence of C [30] and hence expressed the rate equation, Eq. (1) as:

$$-\frac{\partial n}{\partial t} = A'n + Bn^2 \quad (2)$$

Above means that the item An , the radiative recombination exciton density, in Eq. (1), is replaced by Bn^2 . This model suggests that the radiation recombination only occurs between completely unrelated electrons and holes, thus ignoring carrier localization effects and the possibility of exciton recombination [31].

Again, the stability of exciton depends on temperature, electric field, carrier concentration and other factors. At high temperature the exciton will decompose due to thermal excitation. Under the electric field, the exciton effect will be weakened—even abrogated due to electric field ionization. When the carrier concentration is high, the exciton may decompose due to the shielding effect of free charge on the coulomb field. Therefore, exciton

recombination and carrier recombination n should coexist in the polar InGaN/GaN QDs structures. These mechanisms are expressed by An , $A'n$, Bn^2 respectively, where An , $A'n$ and Bn^2 are described as radiative, non-radiative and carrier recombination. Therefore, the rate equation could be expressed as:

$$-\frac{\partial n}{\partial t} = An + A'n + Bn^2 \quad (3)$$

where $n(t)$ represents the carrier concentration. Equation (3) indicates that the free carrier recombination Bn^2 term and the exciton radiation recombination An term are included for the exciton recombination rate equation. It is easy to know that this equation will degrade into the conventional exciton localization model with a single exponential decay solution, in which $(A + A')$ denotes the total recombination rate, if free carrier recombination is ignored and let $B = 0$. To the contrary, it will transform into ABC model proposed by Eq. (2), if localized exciton recombination is ignored and let $A = 0$. We consider the situation as $A, B \neq 0$, and the solution to the Eq. (3) is:

$$n = \frac{A + A'}{\left(\frac{A+A'}{n_0} + B\right)e^{(A+A')t} - B} = \frac{n_0}{\left(1 + \frac{Bn_0}{A+A'}\right)e^{(A+A')t} - \frac{Bn_0}{A+A'}} \quad (4)$$

where n_0 represents the number of carrier concentration at $t = 0$, A , A' and Bn_0 is localized exciton recombination, non-radiative recombination and initial radiative recombination at $t = 0$, respectively. The number of emitted photons $I(t)$ is only related to radiation recombination, and we have $I(t) \propto N(t) \propto An + Bn^2$:

$$I(t) = \beta(An + Bn^2) = I_0 * \frac{\left(1 + \frac{Bn_0}{A+A'}\right)e^{(A+A')t} + \frac{Bn_0}{A} - \frac{Bn_0}{A+A'}}{\left[\left(1 + \frac{Bn_0}{A+A'}\right)e^{(A+A')t} - \frac{Bn_0}{A+A'}\right]^2} * \frac{1}{1 + \frac{Bn_0}{A}} \quad (5)$$

where β , $I(t)$, and I_0 is a proportional coefficient, light intensity at a certain time and light intensity at $t = 0$, respectively. $A + A'$, A , and Bn_0 are fitting parameters. Equation (5), therefore, can be the expression of the TRPL decay curves. Its applications for the analyses of experimental TRPL data are given in next section.

Experimental results and analyses

Figure 2 shows our TDPL spectra of the QDs excited by 376 nm pulse laser—revealing obvious oscillations attributed to the Fabry–Perot (F–P) effect in the film structure. The total structural film thickness ($\sim 4.6 \mu\text{m}$) was calculated from the position of oscillation peaks. The broad peak position around 2.34 eV, was originated from the QDs structure [32]. The peak position shift with temperature in the emission spectra (see: the insert in Fig. 2) suggests the “S-shaped” behavior with a strong evidence of the exciton localization in MQW structures [14]. The temperature-induced shift in the “S-shaped” PL spectra between 14 K \sim 150 K is caused by the change in carrier dynamics with temperature due to inhomogeneity and carrier localization in the InGaN QDs. The results are in good agreement with the observations made in other MQW structures [33, 34]. The slight blue-shift at 180 K may be caused by the systematic error in the PL measurement as weaker PL intensity with stronger Fabry–Perot oscillation making the extraction of real peak position difficult. The observed “S-shaped” behavior in our InGaN/GaN LED samples with QD-like structure suggest the exciton localization as one of the recombination paths. In order to further comprehend the decay processes, we examined the PL decay behaviors at different photon energies.

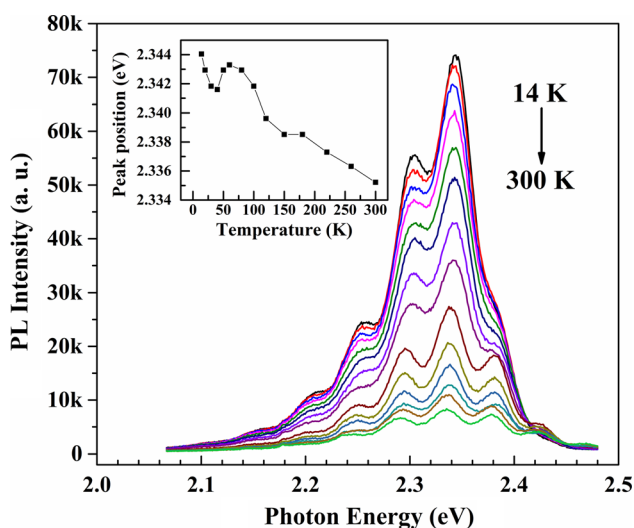


Figure 2 PL spectra and peak position measured at temperature ranging from 14 to 300 K. The inset shows the change of peak position with temperature.

Figure 3a shows the PL decay curves of green QDs sample with different photon energies at low temperatures (14 K). The scatter plots of red, blue, and orange colors correspond to the positions of peak energy, higher energy side, and lower energy side, respectively. Figure 3b shows the PL decay curves of green QDs sample for 2.34 eV emissions at different temperatures. The scatter plots of red, blue, and orange colors correspond to the PL decay curves at 14 K, 100 K, and 150 K, respectively. The black curve shown in Fig. 3a, b is the result of fitting PL decay curves with Eq. (5). A 376 nm pulsed laser was used as the excitation source. The decay curves tested from 10 \sim 300 K and different photon energies were fitted by Eq. (5). Excellent fitting results are obtained for all TRPL decay curves, with deduced rate values as shown below. (See: Figs. 4, 5, 6).

In order to further comprehend the decay processes, we examined the PL decay behaviors at different photon energies. Figure 4 demonstrates the typical results at 14 K, which combines the steady-state PL spectrum and fitted results from PL decays (A , A' and Bn_0) for green QD sample. Based on the above discussion, the shoulder peaks (2.3 eV and 2.25 eV) aside from the PL maximum (2.34 eV) are originating from the F-P interferences. Considering that initial PL intensities for each photon energies are normalized in fitting the decay curves, these interference effects have no influence on the fitting parameter as A , A' and Bn_0 . Here we used Eq. (5) to fit A , A' and Bn_0 for each photon energies around PL maximum.

It can be seen from the results that localized exciton recombination rate A showed a maximum at the lower energy side of the PL main peak. At the higher energy side of the PL maximum, it dramatically descended. On the contrary, Bn_0 showed quick increasing trend only after the photon energy was higher than the PL maximum. These results are correlated with our expectation that among radiative recombination, the localized exciton recombination dominates the lower energy side of the PL maximum because localized states mainly distribute inside InGaN band gap, while the free carrier recombination dominates higher energy side of the PL maximum because the free electrons and holes are distributed in the conduction band and valence band, respectively. Checking the non-radiative recombination, it showed an interesting phenomenon that A' tended to increase from nearly zero following the decrease of A and the

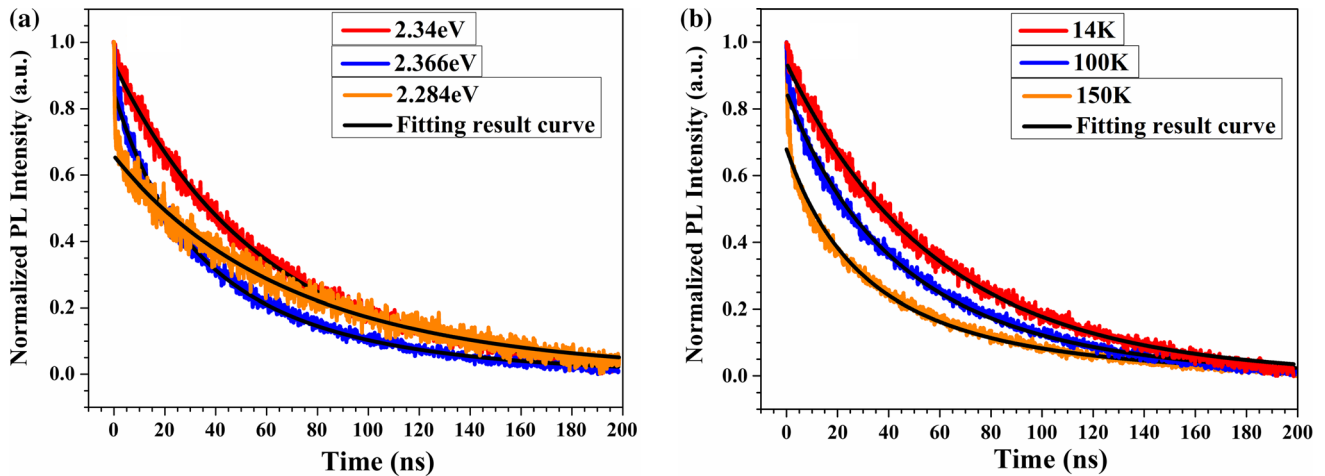


Figure 3 **a** PL decay curves with different photon energy of the InGaN/GaN QDs sample at 14 K. **b** PL decay curves for 2.34 eV emission at tested at 14 K, 100 K and 150 K.

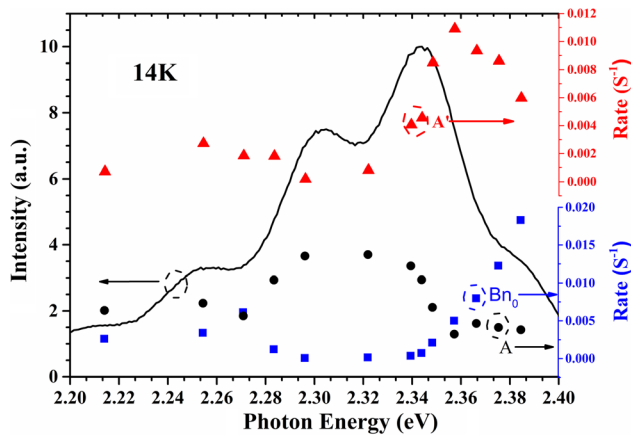


Figure 4 The PL spectrum and model fitted results of green QDs sample at 14 K. The black, red and blue dots denote A, A' and Bn₀, respectively.

increase of Bn₀. These results indicate that free carrier recombination at high photon energy side undergoes a stronger non-radiative counterpart than localized exciton recombination at low photon energy side. This phenomenon can be explained as that localized exciton recombination may more occur at the locations of far away from SRH defects, for instance, inside QDs. On the other hand, the free carrier recombination may occur at the locations with high SRH defect density, for instance, at the interfaces between the grown GaN barrier layer and the layer with InGaN QDs buried. That is caused by QCSE which leads to the tilt of energy band, and free carriers will be restricted in the local minima near the interfaces.

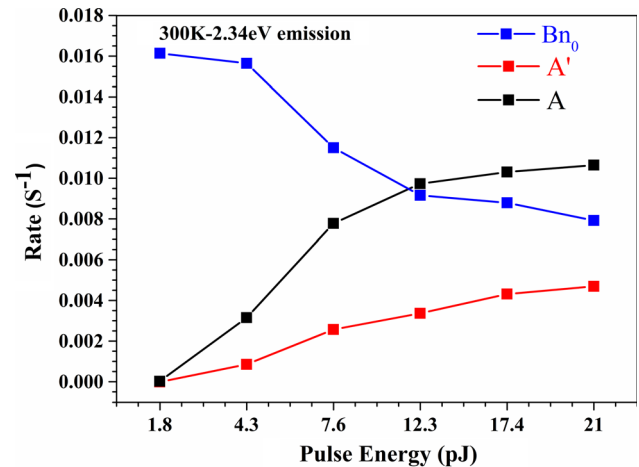


Figure 5 The model fitted results of green QDs samples with different pulse energy injection at 300 K. The black, red and blue dots denote A, A' and Bn₀, respectively.

To shed further light on the dynamic mechanism of the green QDs LED sample, TRPL spectra at different pulse energy injection were investigated. From Fig. 2—the bottom PL spectrum at 300 K, we choose the PL peak of 2.34 eV for the green QDs sample, to perform TRPL measurements on this peak with the injection pulse energy varied from 2.20 to 2.40 eV, and to do the fittings by Eq. (5). Figure 5 shows these model fitting results of A, A' and Bn₀ values, versus the pulse energy at the peak position (2.34 eV) of 300 K. The black, red and blue dots denote A, A' and Bn₀, respectively.

In the higher excitation light pulse energy range, it is found that Bn₀ is larger than A and A' from the typical model fitting. It is worth noting that at low

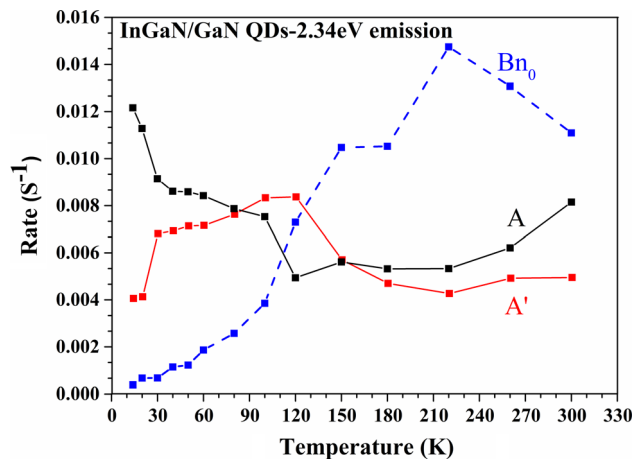


Figure 6 Parameters of the decay curve at peak positions are fitted from the model at each temperature between 14 and 300 K. The black, red and blue dots denote A , A' and Bn_0 , respectively.

pulse energy injection, A approaches 0. This means that most carriers are in the free states at this time and would not be recaptured by the deeply localized states. Because of the separation effect of the built-in field to electrons and holes (QCSE), they were not capable to form excitons. Free carrier recombination dominated the PL processes.

If checking the evolution of A , it can be found that it increased following the rise of injected carrier density. Note that in our TRPL measurements, the output excitation strength was controlled less than 21 pJ per pulse, in other words, the excited carrier density is not larger than 10^9 J/cm² at the LED surface. This can be considered as a weak excitation condition that not all localized states were occupied, and filling effect of the localized states will hardly influence the localized exciton recombination rate. Therefore, here the increase of A with growing injected carrier intensity can be ascribed to the screening of QCSE and decrease of built-in field. This means that the QCSE was screened down by excess electrons and holes, which strongly enhanced the formation of excitons, leading to the increases of the recombination rate of localized excitons. On the other hand, the number of free carriers really involved in the free carrier recombination was dramatically cut down. Note that based on our model, the calculated free carrier recombination rate was not constant by related to carrier concentration. Therefore it appeared that the fitting parameter B decreased due to the competition with A .

Figure 6 shows the temperature dependence of the localized exciton recombination rate (A), non-radiation recombination rate (A') and free carrier recombination rates (Bn_0). A shows a descent trend with increasing temperature in the regime of 14–120 K, which can be ascribed to the enhanced delocalization effect with thermal activations. Also, Bn_0 and A' show an increase trend at the same temperature regime, because the delocalized excitons were broken down into free carriers or trapped by the non-radiative defects. It turned out that A tended to rise from 120 K accompanying with non-monotonic behaviors of Bn_0 and A' in high temperature regime. This phenomenon indicated another competition mechanism due to the delocalization effect with thermal activations, different from the competition of B with A , i.e., the competition between the free carrier recombination and the exciton radiation recombination as discussed in last paragraph. We ascribe it to the increase of thermally excited carrier density.

On a weak excitation condition in our work, the effect from heat induced carriers to QCSE as well as to recombination behaviors may be compatible to the effects from optical injected carriers after temperature beyond some critical point. It can be explained, as increased carrier density partially screened down the built-in field, which leads to the non-monotonic increase of A . Around the temperature of 120 K, the fade away of the built-in field will make free carriers wavefunction less confined in the GaN/InGaN interface region, on which high densities of SRH defects exist. Therefore, A' decreases. But at higher temperature regime above 240 K, thermal activation of the non-radiative process will become dominant. Thus A' rises again. As the data of Fig. 5 was measured at 300 K, at which thermal activation effect will always overwhelm the screening effect, so the decrease of A' cannot be observed.

IQE calculation

Typically, the assumption that the non-radiative lifetime is infinite (i.e., IQE is 100%) at 10 K enables us to determine IQE at RT by normalizing it to the LT integrated PL intensity. However, the assumption of 100% IQE at LT may not be satisfied due to the presence of persistent non-radiative recombination at LT, which is typically manifested at low excitations [35]. Serdel Okur et al. predicted that even at 10 K, a small amount of non-radiative recombination exists

at low excitations through the slopes of the integrated PL intensity versus excitation energy density (carrier density) [36]. From the IQE displayed in Fig. 7, the validity of the above viewpoint is proven at LT. This clearly suggests that it is inaccurate to calculate IQE by normalization of intensity in the temperature-dependent PL measurements.

Based on the above calculation, Eq. (4) can be also expressed as:

$$n = \frac{A + A'}{(\frac{A+A'}{n_0} + B)e^{(A+A')t} - B} = \frac{\frac{A+A'}{B}}{e^{(A+A')t+k} - 1} \quad (6)$$

in which,

$$e^k = \frac{A + A'}{Bn_0} + 1 \quad (7)$$

With the rate Eq. (3) and its solution Eq. (4) obtained previously, the carriers can be clearly divided into radiative, non-radiative and carrier recombination. The respective integration on time are as follows:

$$\begin{cases} \int_0^\infty A n dt = \frac{A}{B} [k - \ln(e^k - 1)] \\ \int_0^\infty A' n dt = \frac{A'}{B} [k - \ln(e^k - 1)] \\ \int_0^\infty B n^2 dt = \frac{A + A'}{B} \left[\frac{1}{e^k - 1} + \ln(e^k - 1) - k \right] \end{cases} \quad (8)$$

and the IQE can be written as:

$$\begin{aligned} \text{IQE} &= \frac{\int_0^\infty A n + B n^2 dt}{\int_0^\infty A n + A' n + B n^2 dt} \\ &= 1 - \frac{A'}{Bn_0} \times \ln \frac{A + A' + Bn_0}{A + A'} \end{aligned} \quad (9)$$

The IQE obtained from Eq. (9) is determined by three parameters: the localized exciton recombination rates (A), non-radiative recombination rate (A') and free carrier recombination rate (Bn_0). The IQE and IQE_0 (initial IQE at $t = 0$) of each temperature are displayed in Fig. 7. Application of Eq. (9) in the peak energy data of green QDs sample suggests the calculated IQE for low temperature/room temperature as 75.3%/72.6% (see: Fig. 7—black dots). As we know, a commonly used formula for IQE_0 is $(A + Bn_0)/(A + A' + Bn_0)$. The calculated IQE_0 for LT/RT is 75.5%/79.5% (see: Fig. 7—the blue colored squares).

It is worth pointing out that these IQE/IQE_0 values were calculated based on the absolute values of recombination rates at the same temperature point, instead of a relative value obtained by comparing ones with values at 0 K, so no extra hypothesis that $\text{IQE} = 1$ at 0 K is required. It is also worthy noted that IQE is closely related to the injected carrier concentration, which relies on excitation condition. Therefore, without providing carrier concentration, it is usually not necessary to discuss IQE, because it can be improved by increasing the carrier concentration. While IQE is generally used to explain the quality of InGaN/GaN QDs crystals, the important thing is to clarify the relationship between radiative recombination and non-radiative recombination for better understanding the carrier recombination mechanism.

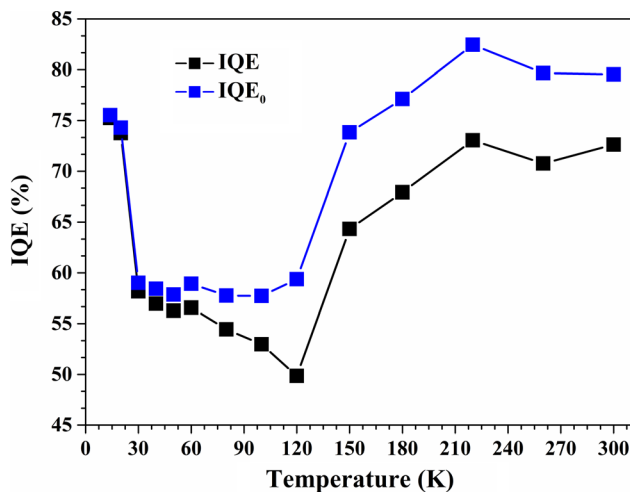


Figure 7 The temperature-relative IQE and IQE_0 of green QDs sample, calculated from the PL decay curve at the energy of PL main peak. The black dots are IQE calculated by Eq. (9). The blue dots are IQE_0 calculated by $(A + Bn_0)/(A + A' + Bn_0)$ which simulates an IQE_0 under a constant carrier concentration n_0 . The nested graph shows the dependence of ΔIQE ($\Delta\text{IQE} = \text{IQE}_0 - \text{IQE}$) on temperature.

Conclusions

In summary, this work reported the comprehensive measurements of the temperature and power variation data for the steady-state photoluminescence (SSPL) and time-resolved photoluminescence (TRPL)

spectra on InGaN/GaN QDs. A novel theoretical model is proposed to explain the non-exponential decay curve of TRPL measurements for InGaN/GaN QDs structures. The model included the localized exciton recombination rate (A), non-radiation recombination rate (A') and free carrier recombination rates (Bn_0) coefficients and applied to the TRPL data of green QDs.

From the power dependence study of A , A' and Bn_0 , our results show that most carriers will not be trapped by deeply localized states at the pulse energy injection of $1.8 \sim 12.3$ pJ, and free carrier combination dominates in the structures. At higher pulse energy injection, the localized exciton recombination is the key process but the contribution of free carrier combination is higher than that of non-radiation recombination, i.e., it still plays an important role. From the temperature dependences of A , A' and Bn_0 , the results show that the non-radiation recombination mainly occurs in certain localized states in the range of $10 \sim 120$ K due to the low recombination rate of free carrier. With the increase of temperature, the regular thermalization of the carriers becomes significant. Combining with IQE results, it is concluded that the thermal activation of the SRH recombination center is affected by the degree of delocalization. The application of the model to IQE calculation is also carried out on InGaN/GaN QDs.

Although the exciton localization effect is enhanced by stronger localized states formed within InGaN/GaN QD structures, the free carrier recombination cannot be ignored. Also, it is found that the hypothesis that there is no non-radiative recombination at LT may not be fully valid. Based on the above conclusions, according to our theoretical model, the relationship between radiative and non-radiative recombination can be explained more comprehensively. The recombination mechanism of carriers in green QDs structure can be revealed more profoundly and this methodology has put forward a new idea to address in solving “green gap” problem.

Acknowledgements

This work was supported by the National Natural Science Foundation of China (No.61367004), the Guangxi Natural Science Foundation (2018GXNSFAA138127), the special funding for Guangxi distinguished professors (Bagui Rencai &

Bagui Xuezheng), and the project supported by State Key Laboratory of Luminescence and Applications (No SKLA-2019-06).

Compliance with ethical standards

Conflicts of interest The authors declare that they have no conflict of interest.

References

- [1] Tawfik WZ, Hyun GY, Lee SJ, Ryu SW, Ha JS, Lee JK (2018) Enhanced performance of GaN-based LEDs via electroplating of a patterned copper layer on the backside. *J Mater Sci* 53:8878–8886. <https://doi.org/10.1007/s10853-018-2177-8>
- [2] Sun H, Park YJ, Li KH, Liu X, Detchprohm T, Zhang X, Dupuis RD, Li X (2018) Nearly-zero valence band and large conduction band offset at AlN/GaN heterointerface for optical and power device application. *Appl Surf Sci* 458:949–953
- [3] Nakamura S (2013) The blue laser diode: the complete story. In: Pearton S, Fasol G (Eds.). Springer, Berlin
- [4] Z. C. Feng (2017) Handbook of solid-state lighting and LEDs. CRC, Taylor & Francis Group, New York
- [5] Feng ZC (2017) III-Nitride materials devices and nanostructures. World Scientific Publishing, Singapore
- [6] Jiang F, Wu X, Mo C, Ding J, Liu J, Zhang J, Wang G, Quan Z, Xu L, Wang X, Zheng C, Pan S, Guo X (2019) Efficient InGaN-based yellow-light-emitting diodes. *Photon Res* 7:144–148
- [7] Su ZC, Wang ZL, Yu JD, Yi Y, Wang MZ, Wang L, Luo Y, Wang JN, Xu SJ (2017) Managing green emission in coupled InGaN QW-QDS nanostructures via nano-engineering. *J Phys Chem C* 121:22523–22530
- [8] Peng L, Zhao D, Zhu J, Wang W, Liang F, Jiang D, Liu Z, Chen P, Yang J, Liu S, Xing Y, Zhang L (2019) Achieving homogeneity of InGaN/GaN quantum well by well/barrier interface treatment. *Appl Surf Sci* 505:144283
- [9] Wang L, Wang L, Yu J, Hao Z, Luo Y, Sun C, Han Y, Xiong B, Wang J, Li H (2019) Abnormal stranski-krastanow mode growth of green InGaN quantum dots: morphology, optical properties, and applications in light-emitting devices. *ACS Appl Mater Interfaces* 11:1228–1238
- [10] Hu L, Ren XY, Liu JP, Tian AQ, Jiang LR, Huang SY, Zhou W, Zhang L, Yang H (2020) High-power hybrid GaN-based green laser diodes with ITO cladding layer. *Photon Res* 8:030279
- [11] Higo T, Kiba S, Chen Y, Chen T, Tanikawa C, Thomas CY, Lee YC, Lai T, Ozaki J, Takayama I, Yamashita A,

- Murayama SS (2017) Optical study of sub-10 nm $\text{In}_{0.3}\text{Ga}_{0.7}\text{N}$ quantum nanodisks in GaN nanopillars. *ACS Photon* 4:1851–1857
- [12] Nippert F, Karpov SY, Callsen G, Galler B, Kure T, Nenstiel C, Markus R, Straßburg M, Lugauer H, Hoffmann A (2017) Temperature-dependent recombination coefficients in InGaN light-emitting diodes: hole localization, Auger processes, and the green gap. *Appl Phys Lett* 109:161103
- [13] Wang Q, Yuan GD, Liu WQ, Zhao S, Liu ZQ, Chen Y, Wang JX, Li JM (2019) Semipolar (1101) InGaN/GaN red-amber-yellow light-emitting diodes on triangular-striped Si (100) substrate. *J Mater Sci* 54:7780. <https://doi.org/10.1007/s10853-019-03473-0>
- [14] Li H, Li P, Kang J, Ding J, Ma J, Zhang Y, Yi X, Wang G (2016) Broadband full-color monolithic InGaN light-emitting diodes by self-assembled InGaN quantum dots. *Sci Rep* 6:1–7
- [15] Tsai SC, Fang HC, Lai YL, Lu CH, Liu CP (2016) Efficiency enhancement of green light emitting diodes by improving the uniformity of embedded quantum dots in multiple quantum wells through working pressure control. *J Alloys Compd* 669:156–160
- [16] Tsai SC, Lu CH, Liu CP (2016) Piezoelectric effect on compensation of the quantum-confined Stark effect in InGaN/GaN multiple quantum wells based green light-emitting diodes. *Nano Energy* 28:373–379
- [17] De S, Layek A, Bhattacharya S, Kumar Das D, Kadir A, Bhattacharya A, Dhar S, Chowdhury A (2012) Quantum-confined Stark effect in localized luminescent centers within InGaN/GaN quantum-well based light emitting diodes. *Appl Phys Lett* 101:121919
- [18] Cho JH, Kim YM, Lim SH, Yeo HS, Kim S, Gong SH, Cho YH (2018) Strongly coherent single-photon emission from site-controlled InGaN quantum dots embedded in GaN nano pyramids. *ACS Photon* 5:439–444
- [19] Schulz S, O'Reilly EP (2010) Theory of reduced built-in polarization field in nitride-based quantum dots. *Phys Rev B* 82:033411
- [20] Ma J, Ji X, Wang G, Wei X, Lu H, Yi X, Duan R, Wang J, Zeng Y, Li J, Yang F, Wang C, Zou G (2012) Anomalous temperature dependence of photoluminescence in self-assembled InGaN quantum dots. *Appl Phys Lett* 101:131101
- [21] Park IK, Park SJ (2011) Green gap spectral range light-emitting diodes with self-assembled InGaN quantum dots formed by enhanced phase separation. *Appl Phys Expr* 4:042102
- [22] Chichibu S, Kawakami Y, Sota T (2000) Introduction to nitride semiconductor blue lasers and light emitting diodes. Talor & Francis, London
- [23] Morel P, Lefebvre S, Kalliakos T, Taliencio T, Bretagnon BG (2003) Donor-acceptor-like behavior of electron-hole pair recombinations in low-dimensional (Ga, In)N/GaN systems. *Phys Rev B-Condens Matter Mater Phys* 68:1–6
- [24] Johnston DC (2006) Stretched exponential relaxation arising from a continuous sum of exponential decays. *Phys Rev B-Condens Matter Mater Phys* 74:1–7
- [25] Li ZC, Liu JP, Feng MX, Zhou K, Zhang SM, Wang H, Li DY, Zhang LQ, Sun Q, Jiang DS, Wang HB, Yang H (2013) Effects of matrix layer composition on the structural and optical properties of self-organized InGaN quantum dots. *J Appl Phys* 114:093105
- [26] Dawson P, Schulz S, Oliver RA, Kappers MJ, Humphreys CJ (2016) The nature of carrier localization in polar and nonpolar InGaN/GaN quantum wells. *J Appl Phys* 119:181505
- [27] Wang L, Hao Z, Han Y, Sun C, Li H, Yang D, Xing Y, Luo Y, Wang Z, Xiong B, Wang J (2017) A novel model on time-resolved photoluminescence measurements of polar InGaN/GaN multi-quantum-well structures. *Sci Rep* 7:1–9
- [28] Li H, Li P, Kang J, Li Z, Zhang Y, Liang M, Li Z, Li J, Yi X, Wang G (2013) Analysis model for efficiency droop of InGaN light-emitting diodes based on reduced effective volume of active region by carrier localization. *Appl Phys Exp* 6:092101
- [29] Zhao CY, Tang CW, Lai BL, Cheng GH, Wang JN, Lau KM (2020) Low-efficiency-droop InGaN quantum dot light-emitting diodes operating in the “green gap”. *Photon Res* 8:750–754
- [30] Fu H, Lu Z, Zhao Y (2016) Analysis of low efficiency droop of semipolar InGaN quantum well light-emitting diodes by modified rate equation with weak phase-space filling effect. *AIP Adv* 6:065013
- [31] Pristovsek M, Badcock TJ, Ali M, Oliver RA, Shields AJ, Zhu T (2016) Radiative recombination mechanisms in polar and non-polar InGaN/GaN quantum well LED structures. *Appl Phys Lett* 109:151110
- [32] Hums C, Finger T, Hempel T, Christen J, Dadgar A, Hoffmann A, Krost A (2007) Fabry-Perot effects in InGaN/GaN heterostructures on Si-substrate. *J Appl Phys* 101:033113
- [33] Feng SW, Cheng YC, Chuang YY, Yang CC, Lin YS, Hsu C, Ma KJ, Chyi JI (2002) Impact of localized states on the recombination dynamics in InGaN/GaN quantum well structures. *J Appl Phys* 92:4441–4448
- [34] Cho YH, Gainer GH, Fischer AJ, Song JJ, Keller S, Mishra UK, Denbaars SP (1998) “S-shaped” temperature-dependent emission shift and carrier dynamics in InGaN/GaN multiple quantum wells. *Appl Phys Lett* 73:1370–1372
- [35] Iwata Y, Oto T, Gachet D, Banal RG, Funato M, Kawakami Y (2015) Co-existence of a few and sub-micron in

homogeneities in Al-rich AlGaN/AlN quantum wells. *J Appl Phys* 117:1–8

- [36] Okur S, Rishinaramangalam AK, Masabih SMU, Nami M, Liu S, Brener I, Brueck SRJ, Feezell DF (2018) Spectrally-resolved internal quantum efficiency and carrier dynamics of

semi-polar (10–11) core-shell triangular nanostripe GaN/InGaN LEDs. *Nanotechnology* 29:235206

Publisher's Note Springer Nature remains neutral with regard to jurisdictional claims in published maps and institutional affiliations.